Revista Brasileira de Agricultura Irrigada
Brazilian Journal of Irrigated Agriculture
ISSN: 1982-7679 (on-line)
v.18, p. 96 - 108, 2024
Fortaleza, CE - www.inovagri.org.br

DOI: 10.7127/rbai.v1801350

WATER DISTRIBUTION CHARACTERISTICS OF DEFLECTOR PLATES USED IN CENTER PIVOT IRRIGATION SYSTEMS

CARACTERÍSTICAS DE DISTRIBUIÇÃO DE ÁGUA DE PLACAS DEFLETORAS EMPREGADAS EM PIVÔS CENTRAIS

Giuliani do Prado[1], Tiago Bueno Braga Coelho[2] Adriano Catossi Tinos[3] , Edmilson Cesar Bortoletto[1] , Denise Mahl[1], Daniela D'Orazio Bortoluzzi[1]

[1] Professor, Department of Agricultural Engineering, Universidade Estadual de Maringá, Campus do Arenito, Cidade Gaúcha - PR, Brazil.
[2] Agricultural Engineer, Faculdade de Engenharia Agrícola, Universidade Estadual de Campinas, Cidade Universitária, Campinas - SP, Brazil.
[3] Agricultural Engineer, Department of Agricultural Engineering, Universidade Estadual de Maringá, Campus do Arenito, Cidade Gaúcha - PR, Brazil.

ABSTRACT: This study aimed to determine the water distribution characteristics of the Asfix spray-sprinkler manufactured by Fabrimar®. In the evaluations, 96 combinations were considered, based on working pressure (103 and 138 kPa), sprinkler height (0.8, 1.6, and 2.4 m), nozzle diameter (4.4 and 5.6 mm), and deflector plates (two rotating and six fixed). The water application rates were measured from radial rows of collectors. The mean application rates were used to determine the wetted radius and the water distribution curves. The distribution curves were normalized and processed with cluster analysis by the K-Means method. Power equations of the wetted radius, as a function of nozzle diameter, working pressure, and sprinkler height, presented coefficients of determination higher than 90%. Four representative water distribution profiles for deflector plates yellow, red, blue, and purple, as well as white, black, gray, and green resulted, respectively, in standard deviations of 0.191 and 0.219. Operating conditions associated with fixed deflector plates tended to present water accumulation at the end of the radial profile. However, rotating deflector plates (yellow and red) provided a decrease in water application rates along the radial profile.

Keywords: rotating plate, fixed plate, radial profile.

RESUMO: O estudo objetivou determinar as características de distribuição de água do aspersor Asfix produzido pela Fabrimar®. Nas avaliações foram consideradas 96 condições dadas por pressão de serviço (103 e 138 kPa), altura de instalação (0,8, 1,6 e 2,4 m), diâmetro do bocal (4,4 e 5,6 mm) e placas defletoras (duas rotativas e seis fixas). As intensidades de aplicação de água foram mensuradas a partir de linhas radiais de coletores. Os valores médios de intensidade de aplicação foram empregados na determinação dos raios de alcance e dos perfis radiais de aplicação de água. Os perfis radiais foram adimensionalizados e submetidos a análise de agrupamento pelo método K-Means. Equações potenciais de raio de alcance, em função do diâmetro do bocal, pressão de serviço e altura do aspersor apresentaram coeficientes de determinação superiores a 90%. Tanto para as placas amarela, vermelha, azul e roxa, como para as de cor branca, preta, cinza e verde, quatro perfis representativos resultaram, respectivamente, em desvios médios de 0,191 e 0,219. Condições operacionais associadas às placas defletoras fixas tenderam a apresentar um acúmulo de água na extremidade final do perfil radial. Todavia, as placas defletoras rotativas (amarela e vermelha) proporcionaram um decréscimo na intensidade de aplicação de água ao longo do perfil radial.

Palavras-chave: placa rotativa, placa fixa, perfil radial.

Protocolo 1350.27-03-2023- Aprovado em 23-10-2024
* Autor correspondente: gprado@uem.br
Editor de área: Ana Nascimento

INTRODUCTION

Food demand due to population growth should be supplied by increasing the cultivated areas and improving crop techniques (WANG et al., 2022; CHARFI et al., 2021). In this context, irrigation is a vital tool for increasing the quantity and quality of crop production. According to the Brazilian capacity for infrastructure, soil, and topography, the country could expand its irrigated areas by 55.85 million hectares (ANA, 2021).

Under automation, with suitable efficiency and uniformity values, center-pivot systems have been widely employed to irrigate large areas (AL-GHOBARI; DEWIDAR, 2021). Over and above the improvement of this irrigation system, high-pressure impact sprinklers have been replaced by spray-type sprinklers that operate at low pressures; this can reduce the amount of energy consumption (HUI et al., 2021).

These low-pressure sprinklers have deflector plates, which can be fixed or rotated (VALENCIA et al., 2019). Rotating-plate sprinklers have presented better water distribution than fixed-plate sprinklers but the latter cost less. Nevertheless, the proper selection of operating combinations can result in similar water application uniformity, regardless of plate type.

The ideal operating arrangement for irrigation systems to be able to reach high uniformity can be set during the project design, based on digital simulations. Therefore, the technical data measured for the water distribution from sprinklers (the water distribution profile), working under distinct operations, are essential (ZHANG et al., 2019).

Rovelo et al. (2019) pointed out that, only a small amount of technical data has been published by sprinkler manufacturers, in the form of water distribution profiles. Therefore, this study aimed to determine representative geometric shapes of the water distribution profile from a sprinkler operating under different configurations of pressure, nozzle diameter, type of deflector plate, and sprinkler height.

MATERIAL AND METHODS

The work was carried out at the Universidade Estadual de Maringá (UEM), Campus do Arenito (CAR) (in Cidade Gaúcha City in the state of Paraná), to evaluate the water distribution patterns of the Asfix sprinkler manufactured by Fabrimar®. This spray sprinkler is composed of a single nozzle and a deflector plate, and it has been recommended for center pivot and lateral movement irrigation systems.

The water distribution patterns were determined for 96 operating combinations, given by: a) two working pressures (103 and 138 kPa); b) two nozzle diameters (4.4 and 5.6 mm); c) three sprinkler heights related to the water collectors (0.8, 1.6, and 2.4 m), and; d) eight deflector plates (Figure 1).

Red rotating plate: angle of 12º		Yellow rotating plate: angle 21º	
Blue fixed plate: concave shape with 36 grooves		Purple fixed plate: flat shape and smooth	
White fixed plate: convex shape with 36 grooves		Black fixed plate: flat shape with 34 fine grooves	
Gray fixed plate: triangular shape with 32 thick grooves		Green fixed plate: flat shape with 24 thick grooves	

Figure 1. Sprinkler deflector plates employed in the water distribution tests.

To measure the water distribution patterns under no-wind conditions, a test bench was set up near the Laboratory of Hydraulics and Irrigation at UEM/CAR. The apparatus used on the test bench were: i) water reservoir; ii) centrifugal pump; iii) lateral line with gate valves, disc filter, and water flow meter; iv) a digital pressure gauge (ranging from 0 to 5 kgf cm^{-2}) and; v) radial rows of water collectors.

Due to the symmetrical shape of the water applied by the sprinkler-wetted circle in no-wind conditions (LIU et al., 2018), only one quadrant of the wetted circle was considered to measure the water sprinkled.

Hence, water collectors of 8 cm diameter and spaced 0.5 m apart were located along seven radial rows (Figure 2). Assuming the quadrant's origin to be at zero degrees (0-90º), the rows 1 (L1) and 7 (L7) were put down at 2.5 and 87.5º, respectively, and the others (L2, L3, L4, L5, and L6) were set apart at an angular distance of 14º10".

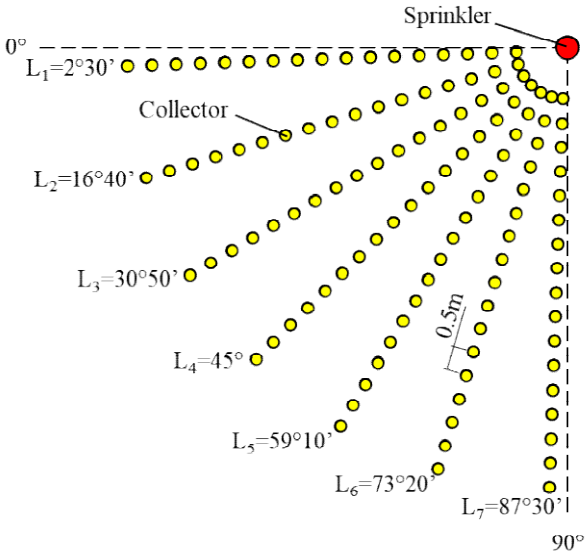

Figure 2. Layout of water collector rows on the test bench to catch the water applied by the sprinkler.

Each of the test durations was one hour long and, within this period, the working pressure was monitored with the digital pressure gauge in the same plane as the sprinkler nozzle. The water volume applied was measured on the flow meter, and forty minutes was considered to be long enough to determine the sprinkler flow rate.

After the test, the water volume in every collector was quantified using a graduated cylinder with 100 cm^3 capacity. The average volume observed in the collectors at the same radial distance from the sprinkler, was divided by the transverse collector area and converted into an application rate (mm h^{-1}).

The application rate data, which was determined to set the mean water distribution curve, was used to compute the sprinkler wetted radius, that represents the most remote point at which the sprayer deposits water at a minimum rate of 0.25 mm h^{-1}, specified in ISO 8026 (ISO, 2009). Collector rows 1 and 4 were discarded due to splashes caused by a concrete pillar and the influence of the sprinkler rod.

The flow rate and sprinkler wetted radius were adjusted by the least squares method under different operating combinations, as described by Equations (1) and (2), respectively.

$$q = a_1 * n^{a2} * p^{a3} \quad (1)$$

$$R = a_4 * h^{a5} * n^{a6} * p^{a7} \quad (2)$$

where: q is the sprinkler flow rate (m^3 h^{-1}); R is the sprinkler wetted radius (m); n is the nozzle diameter (mm); p is the working pressure (kPa); h is the sprinkler height (m), and a_1, a_2, a_3, a_4, a_5, a_6 and a_7 are the fitting coefficients of the equations.

Considering combinations of working pressure (p) and nozzle diameter (n), the decrease of the wetted radius determined by the sprinkler height at 2.4 m was computed by:

$$D_R = \frac{(R_h - R_{2.4})}{R_{2.4}} * 100 = \left[\left(\frac{h}{2.4}\right)^{a5} - 1\right] * 100 \quad (3)$$

where: DR is the decrease in the sprinkler wetted radius (%); R_h is the wetted radius for the sprinkler height h (m); and $R_{2.4}$ is the wetted radius for the sprinkler height at 2.4 m.

With the aim of avoiding volumetric errors in digital simulations (PRADO, 2016), the mean application rate, as a function of radial distance to the sprinkler, was used to estimate the flow rate applied

by the sprinkler at the end of each water distribution test:

$$q_p = \frac{2*\pi}{1000} * \int_0^R i(r)*r*dr \quad (4)$$

where: q_p is the flow rate estimated from the water distribution curve ($m^3\ h^{-1}$); i(r) is the application rate as a function of radial distance to the sprinkler (mm h^{-1}); and r is the radial distance of a water collector to the sprinkler (m).

According to Solomon and Bezdek's (1980) methodology, the water distribution curves were normalized. Thus, the radial distances to the sprinkler were set as a fraction of the wetted radius (Equation (5)) and the application rate was set as a fraction of the average water application rate (Equation (6)).

$$r_d = \frac{r}{R} \quad (5)$$

$$i_d = \frac{i_c * \pi * R^2}{1000 * q_p} \quad (6)$$

where: r_d is the dimensionless radial distance to the sprinkler (-); and i_d is the dimensionless water application rate (-).

The dimensionless water distribution curves were submitted to clustering analysis using the K-Means method described by Solomon and Bezdek (1980). Two clustering analyses were processed, one employing the dimensionless water distribution curves set to the yellow, red, blue, and purple deflector plates (48 curves) and another to the white, black, gray, and green deflector plates (48 curves).

In order to run the clustering analysis, twenty application rates were set for every dimensionless water distribution curve, using the cubic spline interpolation algorithm (BURDEN; FAIRES, 2003). The dimensionless radial distances to the sprinkler were given by Equation (7).

$$r_d = 0.025 + (j-1)*0.05 \quad (7)$$

Where: j is the radial distance index, from 1 to 20.

RESULTS AND DISCUSSION

Average values of the flow rate, coefficient of variation, and flow rate given in the manufacturer's brochure (as a function of nozzle diameter and sprinkler working pressure) are presented in Table 1. The flow rate accuracy can be indicated by the coefficients of variation lower than 1% and the average difference of 1.98% between flows measured and provided by the manufacturer. ISO standard 8026 (ISO, 2009) states that the average flow rate shall not deviate by more than 2.5% from the nominal flow rate.

Table 1. Average flow rate (q_a), coefficient of variation (CV), and flow rate informed by the manufacturer (q_m) as a function of nozzle diameters (n) and working pressures (p).

n (mm)	p (kPa)	q_a ($m^3\ h^{-1}$)	CV (%)	q_m ($m^3\ h^{-1}$)
4.4	103	0.769	0.812	0.750
	138	0.886	0.867	0.850
5.6	103	1.200	0.974	1.210
	138	1.375	0.951	1.370

The 96 flow rate data sets were used to fit a power equation with nozzle diameter and working pressure as independent variables (Figure 3). According to the coefficient of determination obtained, the flow rate outcomes computed by this equation can be explained at 99.83%.

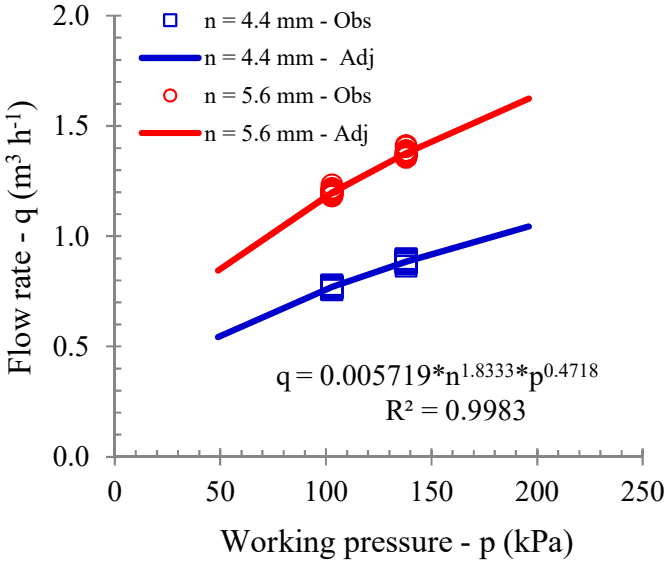

Figure 3. Observed (Obs) and adjusted (Adj) flow rate (q) data as a function of working pressure (p), for sprinklers with nozzle diameters (n) of 4.4 and 5.6 mm.

.

Prado et al. (2021) used flow rate data, measured for 144 combinations of nozzle diameters and working pressures, to fit a power equation, and a coefficient of determination (R^2 = 0.9996) of almost 1.0 was observed. The authors mentioned that the power equation, as a function of nozzle diameter and working pressure, was suitable for modeling the flow rate data. Furthermore, a pressure head exponent equal to 0.5 (LIU et al., 2018), or close to it, has been commonly found for these equations.

Regarding the same deflector plate, combinations of nozzle diameter, working pressure, and sprinkler height resulted in a range of wetted radii (Table 2). Rotating plates (yellow and red) reached a larger wetted radius than the fixed plates, and the flat fixed plate (purple) presented the lowest average value. By evaluating fixed and rotating plate sprinklers, under a pressure of 103 kPa, a sprinkler height of 0.8 m and three nozzle diameters (2.78, 4.76, and 6.75 mm), Jiao et al. (2017) verified wetted radius values ranging from 5.02 to 6.85 m and 4.88 to 7.05 m, respectively.

.

Table 2. Wetted radius range measured in the testing for each deflector plate: maximum (R_{max}), average (R_{ave}), and minimum values (R_{min}).

Deflector Plate	R_{max} (m)	R_{ave} (m)	R_{min} (m)
Yellow	7.846	6.954	6.056
Red	8.150	7.068	6.000
Blue	6.742	5.626	4.583
Purple	5.200	4.403	3.522
White	5.750	4.524	3.013
Black	7.391	5.502	4.004
Gray	7.400	5.911	4.532
Green	7.478	5.521	3.554

Based on the wetted radii measured (as a function of sprinkler height, working pressure, and nozzle diameter), power equations were fitted for each deflector plate type and coefficients of determination higher than 90% were found (Table 3). Concerning the same independent variables, Sayyadi et al. (2014) set wetted radius equations for sprinklers working with fixed deflector plates and observed coefficients of determination from 93 to 96%, in the regression analysis.

Table 3. Wetted radius (R in m) equations and coefficients of determination (R^2) for the deflector plates as a function of nozzle diameter (n in mm), sprinkler height (h in m), and working pressure (p in kPa).

Deflector plate	Equation	R^2
Yellow	$R=2.8181*h^{0.1865}*n^{0.1530}*p^{0.1222}$	0.9779
Red	$R=2.0401*h^{0.1834}*n^{0.1191}*p^{0.2048}$	0.9496
Blue	$R=0.3828*h^{0.1879}*n^{0.3492}*p^{0.4291}$	0.9050
Purple	$R=1.5509*h^{0.2684}*n^{0.2035}*p^{0.1274}$	0.9499
White	$R=0.4722*h^{0.3654}*n^{0.4251}*p^{0.2984}$	0.9594
Black	$R=0.5015*h^{0.3937}*n^{0.6281}*p^{0.2557}$	0.9713
Gray	$R=0.8036*h^{0.3023}*n^{0.3888}*p^{0.2611}$	0.9690
Green	$R=0.2604*h^{0.4106}*n^{0.4121}*p^{0.4643}$	0.9628

By changing the sprinkler height by one meter, an average variation of 1.07 m was found in the wetted radius. Concerning the sprinkler height of 2.4 m, the percentage values of the wetted radius decrease are shown in Figure 4. By bringing down the sprinkler height from 2.4 to 0.8 m, a reduction of -18.5, -18.3, and -18.7% on the wetted radius was computed for the yellow, red, and blue sprinkler plates, respectively. On the other hand, the purple and grey sprinkler with

deflector plates presented decreases of -25.5 and -28.3% on the wetted radius, respectively, while the white (-33.1%), black (-35.1%), and green (-36.3%) deflector plates had the largest reductions.

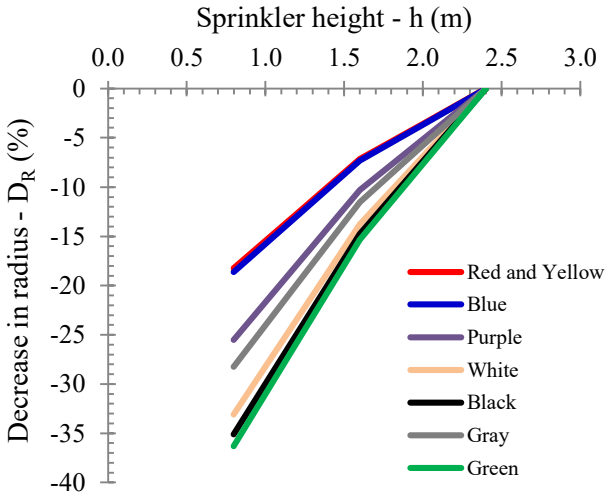

Figure 4. Decrease in the distance of wetted radius for each deflector plate as a function of the sprinkler height.

In the evaluation of a sprinkler with a fixed deflector plate (36 grooves) under combinations of nozzle diameter (4.76 mm), working pressures (50, 100, 150, and 200 kPa), and sprinkler heights (0.5, 1.0, 1.5, 2.0, and 2.5 m), Zhang et al. (2019) achieved a mean variation of 0.72 m in the wetted radius, by altering the sprinkler height by one meter. In addition, a reduction in the sprinkler height from 2.5 to 0.5 m resulted in an average decrease of -39.8% in the wetted radius.

Due to similarities in the dimensionless water distribution curves observed, it was processed as two clustering analyses by the K-Means method (Figure 5). Hence, the dimensionless water curves determined from the yellow, red, blue, and purple deflector plates (48 curves) were used in the first clustering analysis (Figure 5A) and the normalized curves from the white, black, gray, and green deflector plates (48 curves) were processed in a second clustering analysis (Figure 5B).

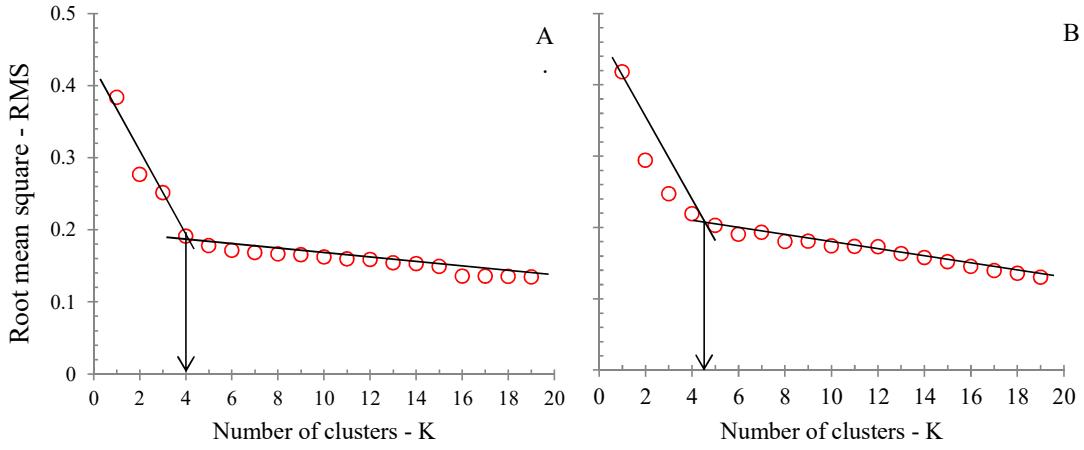

Figure 5. Standard deviation due to K-number of water distribution shapes processed in K-Means analysis for yellow, red, blue, and purple (A) deflector plates and gray, black, white, and green (B) deflector plates.

According to Solomon and Bezdek (1980), the most appropriate number of profiles for representing the water distribution curves can be set at the turning point of the standard deviation curve, as a function of the K-number of clusters. Therefore, the two clustering analyses revealed that four water distribution profiles (K = 4) resulted in standard deviations (RMS) of 0.191 and 0.219, respectively, in the first (Figure 5A) and second (Figure 5B) data sets processed by the K-Mean algorithm.

The geometrical shapes, which represent the dimensionless water distribution profiles from the first (yellow, red, blue, and purple plates) and second (white, gray, black, and green plates) clustering analysis are presented in Figures 6 and 7. In these figures, the vertical bars on the shape curves indicate one standard deviation of the dimensionless water application rate value.

The evident decrease in the water application rate, with respect to the distance from the sprinkler on the water distribution profiles I and II, are presented in Figure 6. However, the water distribution patterns III and IV (Figure 6) provided high application rates at relative distance intervals from 0.2 to 0.8 and 0.2 to 0.5, respectively.

Comparing these water distribution profiles with the geometrical patterns defined by the sprinklers (CHRISTIANSEN, 1942), it can be assumed that geometric profiles I, II, and III resemble Christiansen's theoretical patterns C, A, and E. The water distribution profile IV has no similarity to the water distribution patterns described by Christiansen (1942).

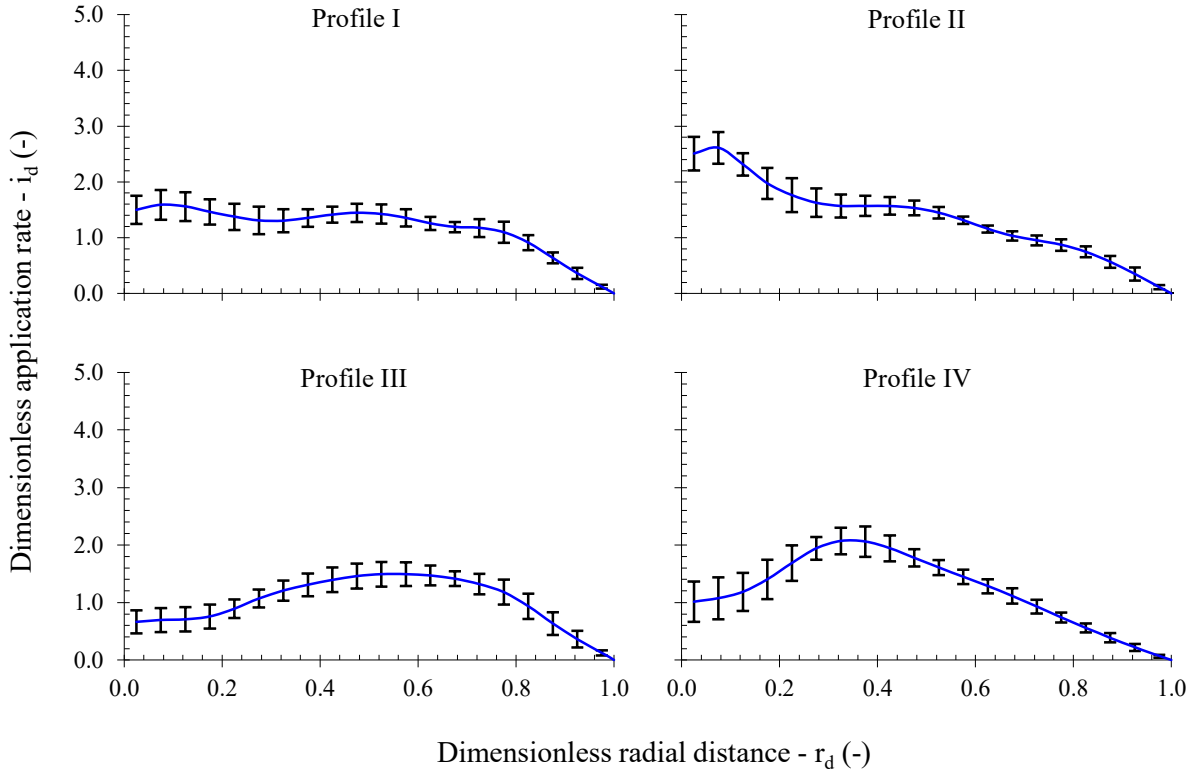

Figure 6. Dimensionless profiles of water distribution curves from the sprinkler working with yellow, red, blue, and purple deflector plates.

The prototypical dimensionless water distribution profiles from the white, black, gray, and green deflector plates (Figure 7) had low water application rate values (less than 1) over the relative distance between 0.0 to 0.6 and, from this point on, the values had sharp increases, which reached dimensionless application rate values of 3, near to the wetted circle edge. According to Rovelo et al. (2019), rotating spray plate sprinklers provide water distribution curves with triangular shapes, while fixed spray plate sprinklers have doughnut or ring shapes.

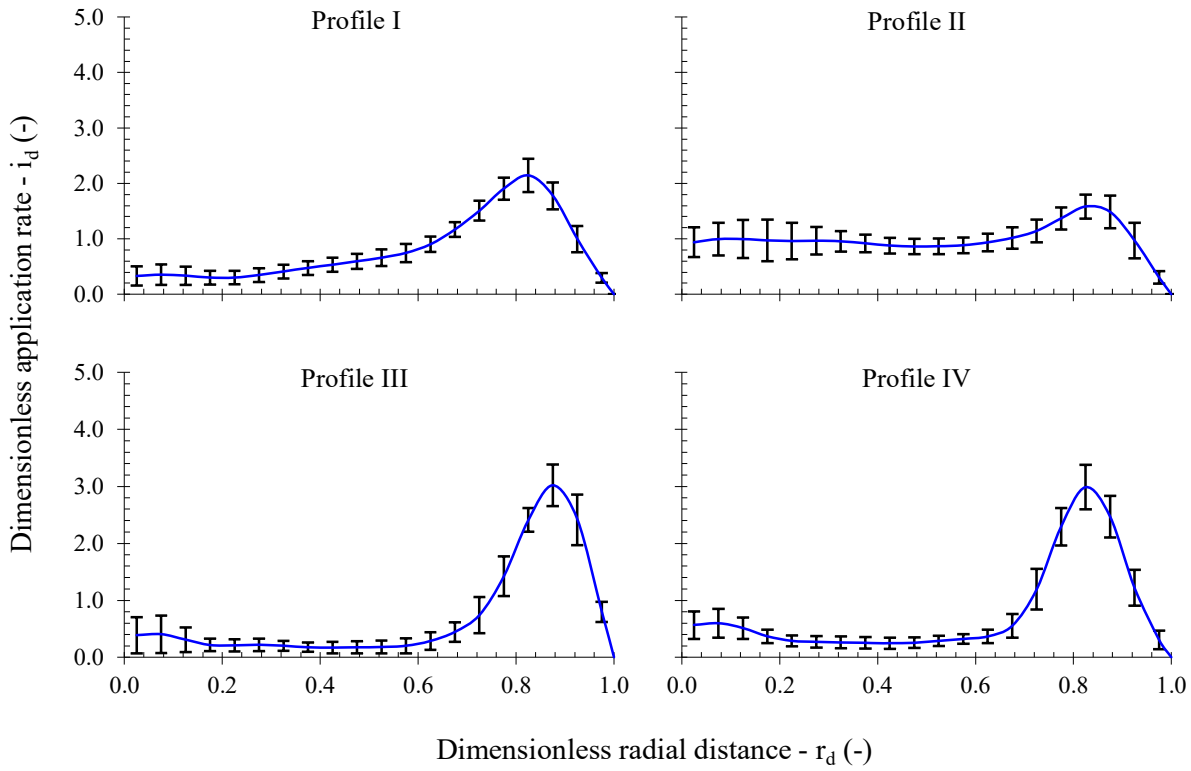

Figure 7. Dimensionless profiles of water distribution curves from the sprinkler working with white, black, gray, and green deflector plates.

Combinations of nozzle diameter, working pressure, and sprinkler height, which define the representative geometric profiles of the water distribution curves, are presented in Tables 4 and 5, respectively, from the first (yellow, red, blue, and purple plates) and second (white, black, gray and green plates) clustering analysis. In Table 4, a high frequency of geometric profiles I and II (Figure 6) are connected to the sprinkler operating with rotating plates (yellow and red). However, profiles III and IV (Table 4) appeared more often for the sprinkler attached to fixed blue and purple deflector plates

.

Table 4. Representative water distribution profiles for the sprinkler with yellow, red, blue, and purple deflector plates as a function of nozzle diameter (4.5 and 5.6 mm), working pressure (103 and 138 kPa), and sprinkler height (0.8, 1.6, and 2.4 m).

Plate	Nozzle Diameter (mm)	Working Pressure (kPa)					
		103			138		
		Sprinkler Height (m)					
		0.8	1.6	2.4	0.8	1.6	2.4
Yellow	4.4	I	II	II	II	II	II
	5.6	I	II	II	I	II	IV
Red	4.4	I	II	I	II	II	I
	5.6	III	I	III	I	I	III
Blue	4.4	III	III	IV	III	III	IV
	5.6	III	III	III	III	I	IV
Purple	4.4	III	IV	IV	III	IV	IV
	5.6	III	IV	IV	III	III	IV

Regarding the sprinkler setup with white, black, gray, or green fixed deflector plates (Table 5), water distribution profiles I and II were observed more often for the white deflector plate, profile II for the green one, and patterns III and IV occurred frequently for black and gray plates. Ouazaa et al. (2014) pointed out that, although fixed deflector plates produce a water distribution curve with a ring shape, the amount of water which accumulates at the wetted circle edge depends on the combination of nozzle diameter and working pressure.

Table 5. Representative water distribution profiles for the sprinkler with white, black, gray, and green deflector plates as a function of nozzle diameter (4.5 and 5.6 mm), working pressure (103 and 138 kPa), and sprinkler height (0.8, 1.6, and 2.4 m)

Plate	Nozzle Diameter (mm)	Working Pressure (kPa)					
		103			138		
		Sprinkler Height (m)					
		0.8	1.6	2.4	0.8	1.6	2.4
White	4.4	I	I	II	I	II	II
	5.6	I	I	II	I	II	II
Black	4.4	III	III	I	IV	III	I
	5.6	IV	III	III	III	III	II
Gray	4.4	IV	IV	III	IV	III	III
	5.6	IV	IV	IV	IV	I	IV
Green	4.4	II	II	II	II	II	II
	5.6	II	II	II	II	II	II

By running laboratory tests for rotating and fixed sprinkler deflector plates and simulating the water distribution uniformity for sprinklers spaced at 1.5, 3.0, and 4.5 m on a lateral line of a center pivot irrigation system, Jiao et al. (2017) determined respective uniformity values from 85.8 to 91.7% and 85.8 to 86.2, for the two plates evaluated. In field water distribution tests of a center pivot under different wind speeds, Lourenço (2018) measured water distribution uniformities from 85.0 to 97.0% and 79.9 to 94.2% for rotating and fixed sprinkler deflector plates, respectively. Therefore, the sprinklers with rotating deflector plates

provide higher uniformity values than the fixed plates.

CONCLUSIONS

Rotating deflector plates result in a larger wetted radius than fixed plates.

When the sprinkler height is altered by one meter, there is a mean variation of 1.07 m on the wetted radius.

Four profiles are sufficient to represent the water distribution curves of a sprinkler working with yellow, red, blue, or purple plates, as well as white, black, gray, or green plates.

Rotating plate sprinklers (yellow and red) should be preferred, as water distribution curves present a decrease in the application rate over the wetted radius.

REFERENCES

AL-GHOBARI, H.; DEWIDAR, A. Z. A comparative study of standard center pivot and growers-based modified center pivot for evaluation uniformity coefficient and water distribution. **Agronomy**, v.11, n.8, p.1-13, 2021. http://doi:10.3390/agronomy11081675

ANA – Agência Nacional de Águas e Saneamento Básico. **Atlas irrigação: uso da água na agricultura irrigada**. 2. ed. Brasília: ANA, 2021. 130 p.

BURDEN, R. L.; FAIRES, J. D. **Análise numérica**. São Paulo: Pioneira Thomson Learning, 2003. 740 p.

CHARFI, I. B.; CORBARI, C.; SKOKOVIC, D.; SOBRINHO, J.; MANCINI, M. Modeling of water distribution under center pivot irrigation technique. **Journal of Irrigation and Drainage Engineering**, v.147, n.7, p.1-10, 2021. http://doi:10.1061/(ASCE)IR.1943-4774.0001571

CHRISTIANSEN, J. E. **Irrigation by sprinkling**. Berkeley: California Agricultural Station, 1942. 124 p. Bulletin, 670

HUI, X.; ZHENG, Y.; YAN, H. Water distribution of low-pressure sprinklers as affected by the maize canopy under a centre pivot irrigation system. **Agricultural Water Management**, v.246, 106646, p.1-10, 2021. http://doi:10.1016/j.agwat.2020.106646

INTERNATIONAL ORGANIZATION FOR STANDARDIZATION. ISO 8026. **Agricultural irrigation equipment – Sprayers: General requirements and test methods**. Geneva, 2009. 18 p.

JIAO, J.; WANG, Y.; HAN, L.; SU, D. Comparison of water distribution characteristics for two kinds of sprinkler used for center pivot irrigation systems. **Applied Science**, v.7, n.4, p.1-17, 2017. http://doi:10.3390/app7040421

LIU, J.; ZHU, X.; YUAN, S.; WNA, J.; CHIKANGAISE, P. Hydraulic performance assessment of sprinkler irrigation with rotating spray plate sprinkler in indoor experiments. **Journal of Irrigation and Drainage Engineering**, v.144, n.8, p.1-7, 2018. http://doi:10.1061/(ASCE)IR.1943-4774.0001333

LOURENÇO, R. D. S**. Modelagem das perdas por evaporação e arraste em emissores de placa defletora fixa e rotativa oscilante na irrigação via pivô central**. 2018. 51 f. Dissertação (Mestrado em Engenharia Agrícola) – Universidade Federal de Viçosa, Viçosa.

OUAZAA, S.; BURGUETE, J.; PANIAGUA, M. P.; SALVADOR, R.; ZAPATA, N. Simulating water distribution patterns for fixed spray plate sprinkler using the ballistic theory. **Spanish Journal of Agricultural Research**, v.12, n.3,

p.850-863, 2014. http://doi:10.5424/sjar/2014123-5507

PRADO, G. Water distribution from medium-size sprinkler in solid set sprinkler systems. **Revista Brasileira de Engenharia Agrícola e Ambiental**, v.20, n.3, p.195-201, 2016. http://doi:10.1590/1807-1929/agriambi.v20n3p195-201

PRADO, G.; COELHO, T. B. B.; TINOS, A. C.; MAHL, D.; BORTOLETTO, E. C. Distribuição de água de microaspersor para diferentes condições operacionais. **Irriga**, v.26, n.4, p.867-883, 2021. http://doi:10.15809/irriga.2021v26n4p867-883

ROVELO, C. O. R.; RUIZ, N. Z.; TOLOSA, J. B.; FÉLIX, J. R.; LATORRE, B. Characterization and simulation of a low-pressure rotator spray plate sprinkler used in Center pivot irrigation systems. **Water**, v.11, n.8, p.1-20, 2019. http://doi:10.3390/w11081684

SAYYADI, H.; NAZEMI, A. H.; SADRADDINI, A. A.; DELIRHASANNIA, R. Characterising droplets and precipitation profiles of a fixed spray-plate sprinkler. **Biosystems Engineering**, v.119, p.13-24, 2014. http://doi:10.1016/j.biosystemseng.2013.12.011

SOLOMON, K.; BEZDEK, J. C. Characterizing sprinkler distribution patterns with a clustering algorithm. **Transactions of the American Society of Agricultural Engineers**, v. 23, n. 4, p. 899- 906, 1980. http://doi:10.13031/2013.34683

VALENCIA, A.; BRIGGS, J.; JACOB, S.; MARSHALL, A. Near field spray measurements for fixed spray plate sprinkler. **Irrigation Science**, v.37, n.1, p.597-609, 2019. http://doi:10.1007/s00271-019-00640-8

WANG, J.; SONG, Z.; CHEN, R.; YANG, T.; TIAN, Z. Experimental study on droplet characteristics of rotating sprinkler with circular nozzles and diffuser. **Agriculture**, v.12, n.7, p.1-21, 2022. http://doi:10.3390/agriculture12070987

ZHANG, Y.; GUO, J.; SUN, B.; FANG, H.; ZHU, D.; WANG, H. Modeling and dynamic-simulation the water distribution of a fixed spray-plate sprinkler on a lateral-move sprinkler irrigation system. **Water**, v.11, n.17, p.1-20, 2019. http://doi:10.3390/w11112296